CERN/LHCC 2001-002
Status Report/RD42
January 12, 2001

Development of Diamond Tracking Detectors for High Luminosity Experiments at the LHC

The RD42 Collaboration

W. Adam[1], E. Berdermann[2], P. Bergonzo[3], F. Bogani[4], E. Borchi[5], A. Brambilla[3], M. Bruzzi[5], C. Colledani[6], J. Conway[7], P. D'Angelo[8], W. Dabrowski[9], P. Delpierre[10], W. Dulinski[6], J. Doroshenko[7], M. Doucet[11], B. van Eijk[12], A. Fallou[10], F. Fizzotti[13], F. Foulon[3], M. Friedl[1], K.K. Gan[14], G. Hallewell[10], S. Han[14], F. Hartjes[12], J. Hrubec[1], D. Husson[6], H. Kagan[14,◇], D. Kania[14], J. Kaplon[15], R. Kass[14], K.T. Knöpfle[16], T. Koeth[7], M. Krammer[1], A. Logiudice[13], R. Lu[13], L. mac Lynne[7], C. Manfredotti[13], D. Meier[15], M. Mishina[17], L. Moroni[8], J. Noomen[12], A. Oh[11], L.S. Pan[14], M. Pernicka[1], L. Perera[7], S. Pirollo[5], M. Procario[18], J.L. Riester[6], S. Roe[15], L. Rousseau[3], A. Rudge[15], J. Russ[18], S. Sala[8], M. Sampietro[19], S. Schnetzer[7], S. Sciortino[5], H. Stelzer[2], R. Stone[7], B. Suter[18], W. Trischuk[20], D. Tromson[3], E. Vittone[13], R. Wedenig[1], P. Weilhammer[15,◇], M. Wetstein[7], W. Zeuner[11], M. Zoeller[14]

[1] *Institut für Hochenergiephysik der Österr. Akademie d. Wissenschaften, Vienna, Austria*
[2] *GSI, Darmstadt, Germany*
[3] *LETI (CEA-Technologies Avancees) DEIN/SPE - CEA Saclay, Gif-Sur-Yvette, France*
[4] *LENS, Florence, Italy*
[5] *University of Florence, Florence, Italy*
[6] *LEPSI, IN2P3/CNRS-ULP, Strasbourg, France*
[7] *Rutgers University, Piscataway, NJ, U.S.A.*
[8] *INFN, Milano, Italy*
[9] *Faculty of Physics and Nuclear Techniques, UMM, Cracow, Poland*
[10] *CPPM, Marseille, France*
[11] *II.Inst. für Exp. Physik, Hamburg, Germany*
[12] *NIKHEF, Amsterdam, Netherlands*
[13] *Univerity of Torino, Italy*
[14] *The Ohio State University, Columbus, OH, U.S.A.*
[15] *CERN, Geneva, Switzerland*
[16] *MPI für Kernphysik, Heidelberg, Germany*
[17] *FNAL, Batavia, U.S.A.*
[18] *Carnegie-Mellon University, Pittsburgh, U.S.A.*
[19] *Polytechnico Milano, Italy*
[20] *University of Toronto, Toronto, ON, Canada*

◇ Spokespersons

Abstract

During the year 2000 the RD42 collaboration was able to achieve considerable progress towards realistic CVD diamond tracking devices which can be used in environments with the highest radiation levels at the LHC. A further improvement of the material developed by De Beers has been achieved with reproducible samples from production reactors with charge collection distances of over 200 μm. Pixel devices equipped with ATLAS and CMS prototype front-end electronics have been successfully tested. in beams. Efficiencies and spatial resolution are close to what is required at LHC. Irradiated strip detectors have been also successfully tested in beams. Further understanding of material properties has been achieved using different techniques of defect characterization. A program aimed at completing this R&D is presented.

1 The RD42 2000 Research Program and Milestones

Vertex detection in LHC detectors requires precise tracking radially close to the interaction regions and in the very forward regions. The integral fluences over the life time of the experiments will exceed substantially 10^{15} particles/cm^2 in these regions. The detector components installed in these regions, both sensor material and front-end electronics, will have to be extremely radiation hard. At present both the CMS and the ATLAS experiment plan to install pixel devices in the innermost layers of their tracking detector. The RD42 collaboration is developing tracking detectors, in particular pixel devices, using CVD diamond material. This material promises to be very radiation hard. The radiation hardness of CVD diamond has been investigated by RD42 up to fluences of 5×10^{15} particles/cm^2. Present results indicate that diamond pixel detectors can be operated with sufficiently high efficiency and spatial resolution close to the interaction region for many years of LHC operation at design luminosity. The availability of very radiation hard detector material and electronics will be of great importance in view of possible future luminosity upgrades for the LHC.

1.1 The LHCC Milestones

At its meeting on the 17. Feb. 2000 the RD42 project was approved with its program to be completed by the end of 2000 [1]. Emphasis was given to beam tests of existing pixel detectors equipped with electronics adequate for LHC experiments. The research program proposed by RD42 for 2000 included [2]

- testing of LHC pixel detectors with ATLAS and CMS electronics,
- finalization of the geometry and metallization of LHC pixel sensors,
- finalization of LHC specific electronics performance for diamond trackers.

Although highly attractive, CVD diamond has three properties that need to be addressed before diamond pixel detectors are viable. Foremost is to understand the effect of the signal size which with full charge collection is approximately half that of silicon. Second is to understand the effects of the material being polycrystalline. Finally the material must be reproducible in its electronic properties, especially charge yield, from production reactors before any orders or realistic pricing can be obtained.

1.2 Summary of Milestone Progress

Using CVD diamond samples from production reactors our work has proceeded on the development of pixel diamond sensors. Electronics with suitable noise and suitable threshold performance have recently become available to us from both ATLAS and CMS. This coupled with the development of a number of large collection distance samples has allowed us to vigorously pursue the development of truly bump-bonded diamond pixel sensors. This work has been performed in collaboration with the groups developing front end electronics for both ATLAS and CMS.

Fig. 1 shows one of the recent diamond pixel sensors with the pixel metallization pattern for CMS. The pixel cells are made of Ti/W, metallized on the diamond surface with a size of 100×100 μm^2. The sharp lithography gives uniform and clean pixel cells over an area of (1×1) cm^2. The photo also shows a few of the deposited indium bumps on the pixels. Fig. 2 shows a side view of the detector and the bump bonding to the readout chip.

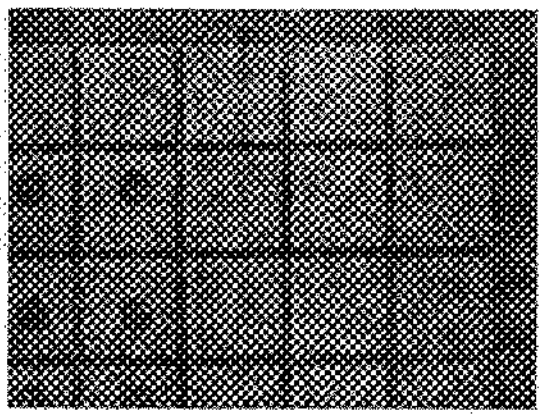

Figure 1: Photograph of the top view of a CMS diamond pixel sensor showing the pixel pattern.

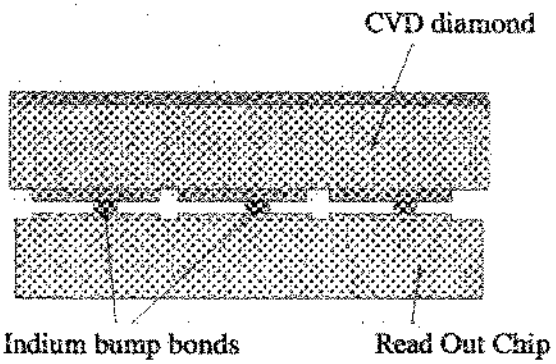

Figure 2: Schematic side view of a CMS pixel detector showing the position of the bump bonds.

The results of beam tests at CERN for these devices yielded position resolution slightly better than digital and the same as that measured in a corresponding silicon pixel detector tested simultaneously. Efficiencies above 90 % have been achieved. The next generation of pixel detectors will use the newly available larger collection distance material (charge collection distance of about 250 μm) and should yield a pixel detector suitable for applications at the LHC.

The development of new diamond material came about as a result of a series of material studies. The primary result of this work showed that our understanding of the growth processes was correct and a clear path to higher quality diamond could be pursued. A decision to pursue such a research program was made during the year and has begun. We expect the first results of this work in mid 2001.

Finally, we continued our irradiation studies of CVD diamond. The performance of diamond strip detectors after irradiation was evaluated in beam tests. Planned tests with strip detectors equipped with a fully radiation hard readout chip (SCTA) produced in the DMILL technology could not be carried out due to late delivery of the chip. A more detailed description of the progress in 2000 is presented in the following sections.

2 Progress on the Improvement of CVD Diamond

Over the last few years, we have worked closely with the De Beers Industrial Diamond Division [3] to achieve major improvements in the charge collection distance and uniformity of CVD diamond.

- CVD diamond purchased from production reactors now regularly exceed 200 μm charge collection distance.
- New 'avenues' of research are being pursued by De Beers for greater than 200 μm charge collection distance. This research will be carried out with RD42 in 2001.
- Research continued on lapping and uniformity in order to gain understanding and improvement in electronic quality.

De Beers presented their plans to the CERN community in a technical presentation in March 2000.

This past year we characterized approximately 30 new diamond samples from production reactors. In previous years the diamond from production reactors was not of the same quality as that from research reactors. The measured pulse height distribution, using a ^{90}Sr source, of two typical samples as-received from the manufacturer is shown in Fig. 3. To obtain this distribution we metallized the diamond with circular electrodes on each side. Operating at an electric field of 1 V/μm we observe a Landau distribution well separated from zero. We also observe that the charge collection is symmetric with applied voltage. The most probable charge is $\approx$ 5500 e and 99 % of the distribution is above 2000 e.

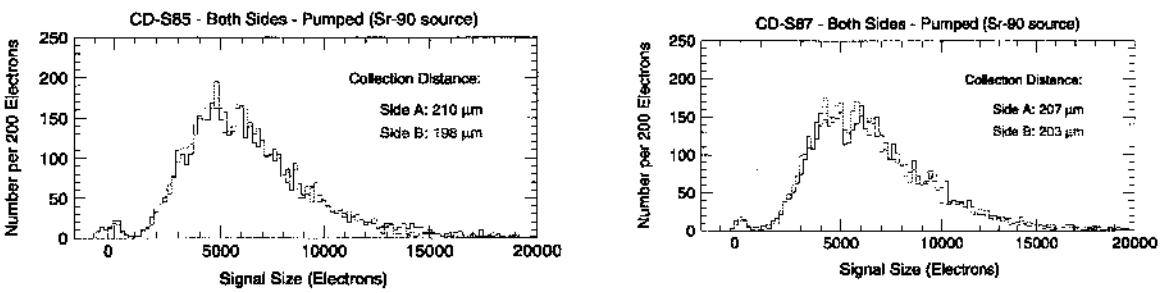

Figure 3: Charge signal from recent production reactor diamond samples measured using a ^{90}Sr source in the laboratory. No cuts to the data have been applied.

From the mean value, $\langle Q \rangle$, of the signal spectrum one derives the charge collection distance

$$\bar{d} = \frac{\langle Q \rangle \ [e]}{36 \ e/\mu\text{m}} \tag{1}$$

where 36 e/μm is the number of electron-hole pairs generated by a minimum ionizing particle along 1 μm in diamond. The charge collection distance of 210 μm in CDS-85 corresponds to a mean charge of 7560 e.

Fig. 4 shows the charge collection distance in De Beers CVD diamond samples since 1995. In the course of our work with De Beers the charge collection distance improved from several 10 μm to over 200 μm in production reactors.

Progress has been made in the understanding of the carrier drift length across the diamond bulk. Fig. 5 shows the charge collection distance measured in two CVD diamond samples as a function of the thickness after thinning on the growth side and on the nucleation side. We find that material removal from the growth side decreases the charge collection distance. The measurements from successive material removals on the growth side can be fit by a straight line indicating that the carrier drift length increases linearly from the nucleation side to the growth side. The intersection at zero gives the carrier drift length on the nucleation side of the diamond. We also find that material removal from the nucleation side improves the charge collection distance. However, charge collection distance must decrease again after a certain amount of material has been removed from the nucleation side. Hence there must be a thickness where the charge collection distance reaches a maximum.

In order to achieve a most reliable characterization of diamond detector samples a new characterization station has been setup at CERN. Fig. 6 shows a photograph of the new setup. A CVD diamond sample can be seen in the center of the picture. A source is fixed underneath the sample. A similar station has been installed at De Beers. The new setup was motivated by the need of having various users be able to characterize samples. Charge collection measurements are usually performed by 3 institutes of RD42 in order to compare

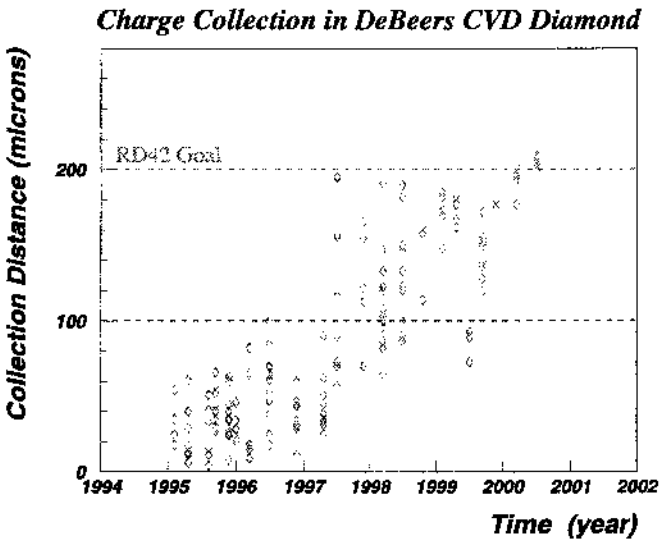

Figure 4: Charge collection distance in De Beers CVD diamond samples since 1995.

results on samples. The CERN characterization station has also been used for measuring CdTe crystals used for LHC luminosity measurements.

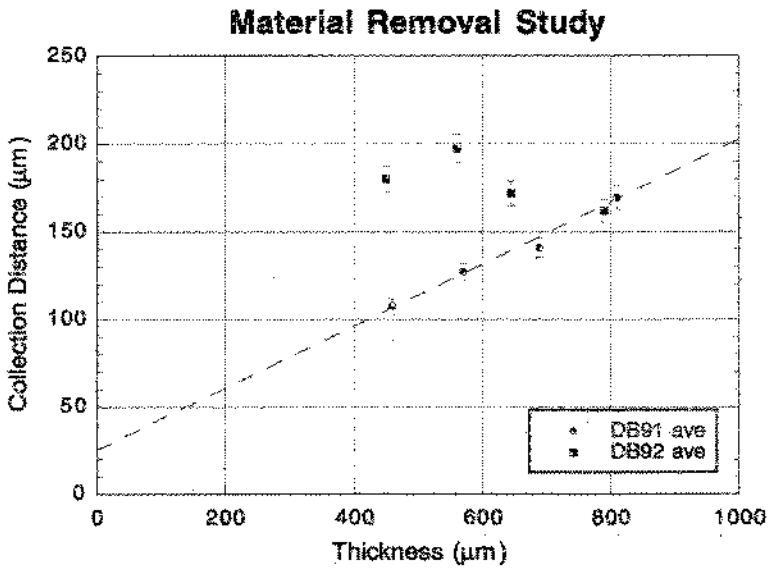

Figure 5: Thinning of two CVD diamond samples (DB91 and DB92). The charge collection distance measured as a function of the thickness after thinning on the growth side of DB91 and on the nucleation side of DB92.

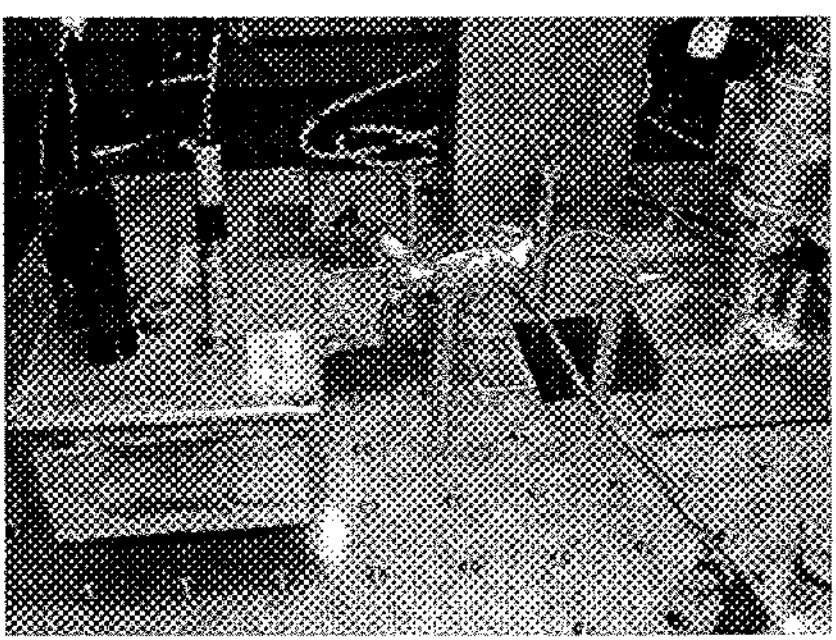

Figure 6: Photograph of the new diamond characterization station at CERN. A CVD diamond sample can be seen in the center of the picture.

3 Results from Diamond Strip Detectors

After characterization of diamond samples using the ^{90}Sr in the lab, the electrical contacts were removed and the samples were patterned with strips or pixels in order to test them as trackers in particle beams. Tests with strips are essential on new materials to understand charge collection, charge sharing and material uniformity. Detailed work on the diamond material is easier achieved on strip- than on pixel detectors. The tests on strips were normally done using 'easy-to-use', low noise VA readout electronics [4]. VA readout was chosen since it allows one to focus on the diamond detector material.

All beam tests were performed using a silicon beam reference telescope [Fig. 7] consisting of 8 planes of silicon strip detectors. Diamond strip or pixel detectors were mounted inside the telescope. The telescope allows one to measure the intersection of the track with the diamond detector with a precision of about 1 μm [5].

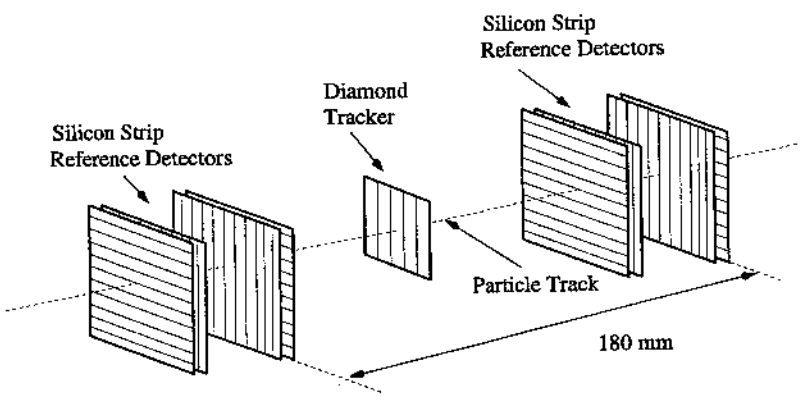

Figure 7: Schematic view of the silicon beam reference telescope.

Table 3 lists the beam tests which were carried out in the year 2000. A total of 12 strip-, 3 CMS pixel- and 1 ATLAS pixel-detector were tested.

testbeam month in year 2000	location	purpose
June	SPS/X7A (parasitic to LHCb/Velo)	6 strip detectors 2 CMS pixel detectors
June/July	SPS/X5A (parasitic to CMS Tracking)	2 CMS pixel detectors
July/Aug.	SPS/H8 (ATLAS Pixel test)	1 ATLAS pixel detectors
Aug.	SPS/H2 (parasitic to CMS Pixels)	2 CMS pixel detectors
Aug.	SPS/X5A (RD42)	7 strip detectors
Nov.	PS/T7 (parasitic to NA58/COMPASS)	3 CMS pixel detectors

Table 1: Beam tests at CERN with CVD diamond detectors in the year 2000.

3.1 Beam Test Results from a Diamond Strip Detector

Extensive beam tests have been carried out in the year 2000 using the setup and experience from previous tests [6]. All diamond strip sensors tested in 2000 had a 50 μm strip pitch at 25 μm strip width. The strips were made of Cr/Au where chromium forms a carbide after annealing and gold provides a conductive protection against oxidation and allows wire-bonding. About 80 strips were read out by low noise VA electronics were the channel noise

was about 100 e ENC. Each detector had a corner with a rectangular contact which allowed characterization using a ^{90}Sr source. Fig. 8 shows the charge signal distribution measured from a recent diamond using a ^{90}Sr source. The sample had a thickness of 470 μm and was biased with 470 V such that the internal electric field was 1 V/μm. This diamond was obtained from a production reactor and is comparable with previous results on diamonds produced in research reactors. It can be seen that the signal distribution is separated from zero with more than 99 % of the entries above 2000 e. The mean value and most-probable values are 7740 e and 5500 e from which the charge collection distance of 215 μm can be derived [Eq. 1].

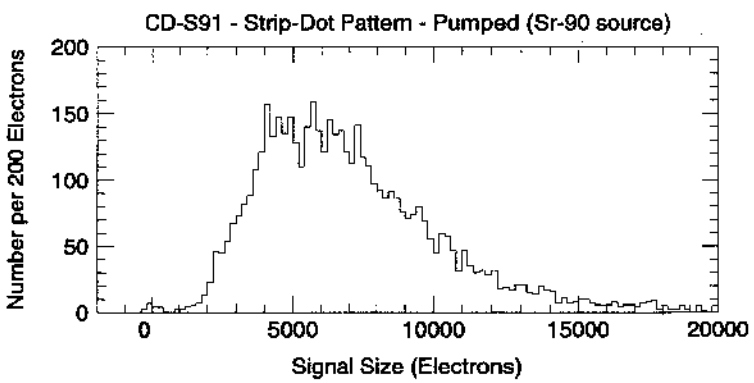

Figure 8: Charge signal distribution in CVD diamond CDS-91 measured at 1 V/μm using a ^{90}Sr source.

Fig. 9 shows the signal distribution measured in the beam. The signal was obtained by adding the charge measured on strips nearest to the intersection of the track given by the reference telescope (transparent analysis method). The distribution of the charge from two and four strips nearest to the track is shown where the charge is given in units of the noise measured on a single strip. The distribution for two (four) strips peaks a 35 (42) and has a a mean value of 50 (60). It can be seen that the charge collected on four strips is larger than on two strips. This observation is likely due to charge trapping inside the bulk such that the time integral over the induced current on adjacent strips does not cancel to zero. Using a channel noise of 100 e to 120 e one derives a mean value of 6000 e to 7200 e on four strips which is smaller the mean signal measured on the same diamond using the ^{90}Sr source. In order to compare the charge signal from dots with the signal from strips we use 4 strips since they cover a larger area than just 2 strips. We note that the analysis uses fiducial regions on the diamond. Regions where two strips were shorted together due to faults during contact fabrication are excluded. Also regions near the corners of the diamond and a few microns near the end of the strips were excluded.

Fig. 10 shows the residual distribution of the same diamond in the beam. The residual is the difference between the position of the track as measured by the reference telescope and the position of the hit as measured by the diamond detector. The 2-strip center-of-gravity method was used to measure the position in the diamond detector. The residuals are normal distributed around zero. The spatial resolution was obtained from the standard deviation of 15.6 μm of a Gaussian fit to the data. This resolution is slightly worse than what was seen on other good diamond strip detectors. The resolution may improve on future detectors from production reactors.

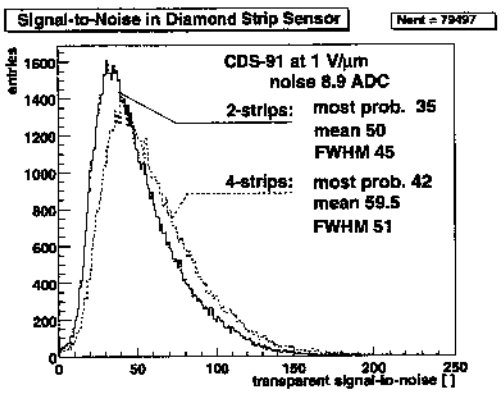

Figure 9: Transparent charge signal-to-noise distributions on 2-strips (solid line) and on 4-strips (dotted line).

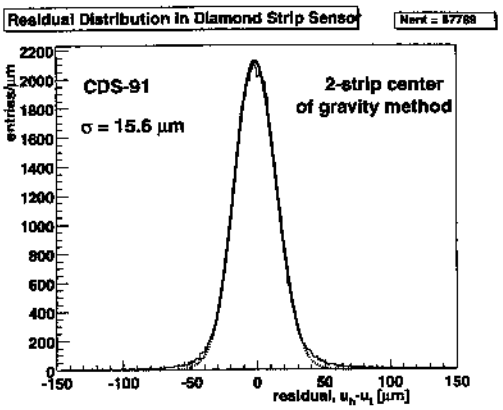

Figure 10: Residual distribution using the 2-strip center of gravity method. The distribution is fitted by a Gaussian function.

3.2 Performance after Proton Irradiation

While results on proton irradiated diamond samples with large circular contacts were reported previously [2] we were studying the performance of proton irradiated diamond strip sensors. The irradiations were performed using 24 GeV/c protons from the Proton Synchrotron at CERN where details of the irradiation can be found in reference [7, 8].

The diamond which was irradiated was one of the best grown in a research reactor. The data for various number of strips before irradiation were shown in reference [2]. Fig. 11 shows the transparent 2-strip signal-to-noise distributions measured on a diamond sensor in beam tests before and after irradiation with fluences of 1×10^{15} p/cm^2 and 2.2×10^{15} p/cm^2. While the strip contacts before and after irradiation with fluences of 1×10^{15} p/cm^2 were unchanged the contacts were replaced after a fluence of 2.2×10^{15} p/cm^2 and then characterized in the test beam. At 1×10^{15} p/cm^2 we observe that the shape of the signal-to-noise distribution is narrower than before irradiation and entries in the tail of the distribution appear closer to the most probable signal. At 2.2×10^{15} p/cm^2 and after re-metallization we observe essentially the same signal-to-noise distribution as at 1×10^{15} p/cm^2 indicating that very little further damage occured to the diamond bulk. The most probable signal-to-noise was 41 before irradiation and 35 at 1×10^{15} p/cm^2 and also at 2.2×10^{15} p/cm^2. We find a reduction of maximum 15 % in the most probable signal-to-noise after irradiation with 2.2×10^{15} p/cm^2. The noise was measured to remain constant at each beam test. Since the beam test with the detector irradiated with a fluence of 2.2×10^{15} p/cm^2 used new contacts the observed decrease of 15 % is attributed to damage in the diamond bulk.

Fig. 12 shows residual distributions before and after irradiation at 1×10^{15} p/cm^2 and 2.2×10^{15} p/cm^2. We observe that the spatial resolution improves from (11.5 ± 0.3) μm before irradiation to (9.1 ± 0.3) μm at 1×10^{15} p/cm^2 and to (7.4 ± 0.2) μm at 2.2×10^{15} p/cm^2. At present there is no clear explanation for this effect. The spatial resolution of nearly 7 μm with a detector of 50 μm strip pitch is comparable to results obtained with silicon detectors.

4 Diamond Pixel Detectors

During the past year, we have initiated test beam studies to determine both the hit efficiency and spatial resolution of diamond pixel detectors configured in both the ATLAS and CMS geometries and readout with the current ATLAS and CMS prototype readout chips.

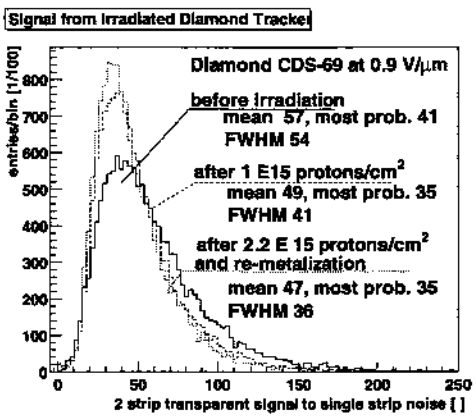

Figure 11: Transparent 2-strip charge signal-to-noise distributions before (solid line), after proton irradiations with 1×10^{15} p/cm^2 (dashed line) and after 2.2×10^{15} p/cm^2 (dotted line).

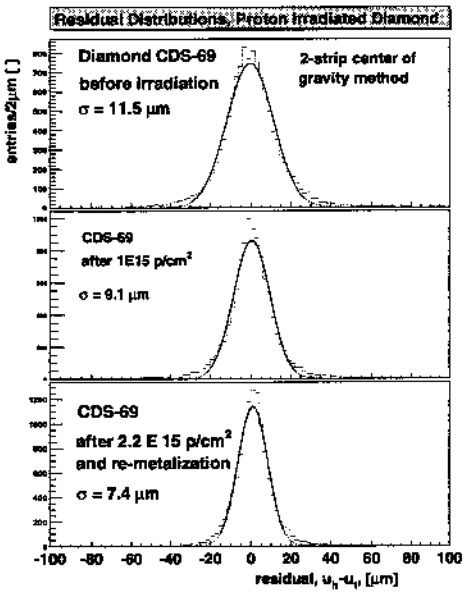

Figure 12: Residual distributions measure before and after proton irradiations.

4.1 Progress on ATLAS Pixel Prototypes

Our first bump-bonded diamond pixel prototype was assembled with an early version of the ATLAS readout chip in 1998. The results from this indium bump-bonded detector were published in a NIM article in 1999 [9]. Since that time we have pursued various bump-bonding and readout chip options in an attempt to improve the overall efficiency of our devices.

Over the last year and a half we have fabricated several ATLAS pixel prototype sensors on 1×1 cm^2 CVD diamond samples [2]. The pixel pattern was fabricated to accommodate the ATLAS pixel readout chips with 18 columns and 156 rows. The column pitch was 400 μm, the row pitch was 50 μm. We have focused on titanium/tungsten metallization, similar to that used with our first prototype. The titanium makes a good carbide bond with the diamond - minimising charge build-up in the diamond bulk while the tungsten is a suitable cover-metal facilitating electrical contact with the bonding material.

In that last nine months our efforts to make an ATLAS pixel prototype have concentrated on using the ATLAS FE-C readout chip. The bump-bonding was performed at IZM, in Germany (one of the candidates for the production bonding of the ATLAS silicon modules), where they use a lead-tin solder b[illegible]ping procedure. The first attempt to bond a diamond with this process (in the autumn o[illegible]1999) yielded only a single column of viable bonds. We re-metallized the same diamond sample and a second bonding was attempted in March 2000. This resulted in about one third of all pixels on the detector being successfully connected. The pattern of connections indicates some systematic failure of adhesion over the other two-thirds of the detector. One possible explanation for this is the thermal expansion mis-match between the diamond sensor and the silicon readout chip when the solder bonds are flowed at 240°C. IZM currently has two other detector quality diamond sensors and is considering process improvements to achieve fully efficient bonding.

4.1.1 Test Results on ATLAS FE-C Prototype

A series of measurements on this diamond pixel prototype bonded to an ATLAS FE-C readout chip have been performed by our ATLAS colleagues from the University of Bonn [1]. Bench tests using a source and charge-injection show that roughly one-third of the detector have viable bonds. Fig. 13 shows the cross coupling in the sensor measured by charge injection into a channel and measuring the signal in an adjacent channel. In one third of the channels the injected charge could be measured indicating a good contact between the detector and the readout. Apparently the other part of the detector was not bonded. Fig. 14 shows the distribution of hits measured using tracks in the particle beam. The hits are seen in channels which are bump-bonded to the detector.

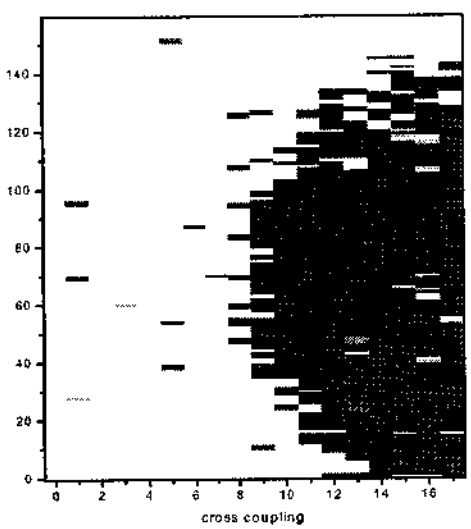

Figure 13: Distribution of hits in pixels measured by charge injection into a neighbour pixel.

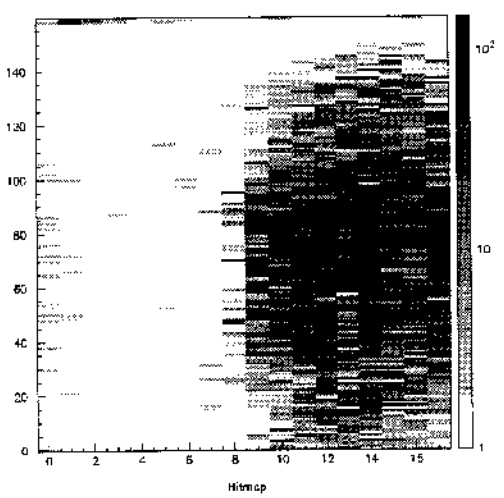

Figure 14: Distribution of hits in pixels measured from charged particles in the testbeam.

The device was tested in a beam at CERN in July 2000. The distribution of the residuals for the 50 μm readout pitch are shown in Fig. 15. The spatial resolution (20 μm) is consistent with our expectations for such a detector given the relatively large fraction of single pixel hits.

While this diamond sample has been measured to yield an average signal of 7000 electrons per minimum ionising particle, it is only capable of doing this in its "pumped" state – after exposure to a few kilo-rad of ionising radiation. The FE-C chip is still produced in a rad-soft technology, thus we are prevented from "pumping up" the diamond before testing the pixel prototype in a beam. In the "un-pumped" state this diamond is expected to produce 4500 electrons average charge for minimum ionising particles. We observe an average of 4200 electrons in the pixel device.

One marked improvement in the FE-C readout chip, relative to the chip used in the previous ATLAS pixel prototype is that the threshold can be set significantly lower. This when combined with a 30 % increase in charge available in the new diamond samples resulted in an increase in the overall efficiency of the well-bonded region of the detector from 40 % (as shown in reference [9]) to over 80 %. However, approximately 1/4 of the hits have significant time-walk ending up one or more beam crossings before or after the passage of the charged

[1] M. Keil, P. Fischer, S. Meuser, N. Wermes, University of Bonn, Physikalisches Institut, Nussallee 12, 53115 Bonn, Germany.

particle of interest. In an LHC application these hits might be lost. The only cure for these losses is to increase the signal size in the diamond – something that occurs naturally when we will expose the device to a few kilo-rad of ionizing radiation.

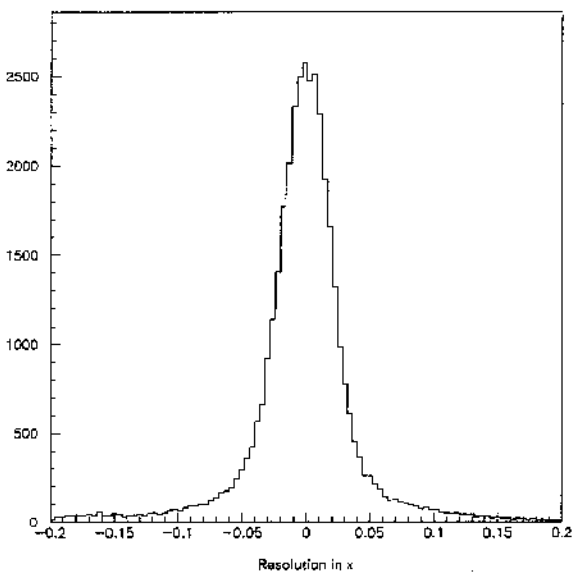

Figure 15: Distribution of the residuals measured in the testbeam.

4.2 Diamond Pixel Sensors for CMS

In a series of tests this past year at the CERN SPS and PS, three CVD diamonds bump-bonded to CMS prototype readout electronics were tested. The diamonds were from the most recent set of samples delivered by De Beers. They were grown to over 1 mm thickness with material removed from the nucleation side reducing the thickness to 500 microns. The pieces were 1 cm×1 cm in area. The charge collection distance of each diamond was determined using a 5 mm diameter circular electrode and a ^{90}Sr beta source. The charge collection distances were between 200 and 250 microns for the three diamonds when biased at 1 V/micron.

In order to test these diamonds with CMS readout electronics, diamond sensors were prepared with a pixel pattern of 22 columns × 32 rows and 125 micron × 125 micron pitch. (The current CMS design calls for 150 micron × 150 micron pixels. However, the best currently available readout chip uses the old design of 125 microns × 125 microns.) The diamonds were metallized by sputtering Ti/W over both surfaces and acid etching one surface to produce the pixel pattern. The pixels were then indium bump-bonded to the Honeywell version (RICMOS IV process) of the CMS PSI30 pixel readout chip. This chip has a double-column architecture consisting of 11 double-columns and 32 rows of pixel unit cells. Each cell contains a charge-sensitive preamplifier with a 30 fF feedback capacitor and a shaper amplifier with a peaking time adjustable around 30 ns. Each cell has a test input capacitor of 1.68 fF for calibration. The amplified signal is brought to a comparator with threshold individually adjustable for each cell. The output of the comparator sets a flip-flop which activates storage of the analog pulse heights onto switched capacitors for all of the pixels within the double column following an adjustable hold time. When the chip receives an external trigger of the appropriate latency, the entire double column of pixel pulse height information is readout. The chip has an intrinsic noise of 80 electrons. In the test beam measurements, a noise of 110 electrons and a threshold setting of 1000 to 1200 electrons were achieved.

The detectors were tested in beams at both the SPS and PS using a tracking telescope consisting of four horizontal and four vertical planes of silicon micro-strip detectors. Tracks were extrapolated with a precision better than 2 μm in the high energy π beam at the SPS. In the PS beam of 15 GeV/c protons, the track projection resolution was limited by multiple scattering and was about 5 microns. Due to improvements in the readout system, the pixel noise achieved at the later PS running was more than a factor of two better than that at the earlier SPS running. Our best results are, therefore, from the PS data and these are what we present here. For all measurements, the diamond sensor was biased at a field of 1 V/μm. The PSI30 readout chip is rad hard so that, unlike the case of the ATLAS pixel tests, the diamonds were fully "pumped" with several kilo-rad of ^{90}Sr exposure before being tested in the beam. We collected data on all three of the diamond pixel detectors. The results were all similar and we present here the data for the detector on which we accumulated the most statistics.

4.2.1 Pulse Height

The pulse height distribution for the pixel to which a charge track extrapolated is shown in Fig. 16 for events with tracks that passed through the active area. The measured calibration corresponds to 13 electrons of collected charge per ADC count. The readout chip gain is nonlinear for input signals greater than 10000 electrons and saturates at an input signal of about 12000 electrons causing the peak seen at around 900 ADC counts. The most probable peak value of 250 and mean of 402 ADC counts are substantially below the values measured for ^{90}Sr with a 5 mm diameter dot electrode. This discrepancy is primarily due to charge spreading onto several pixels. Most of this charge spreading is likely due to partial trapping within the diamond. In the case of the dot electrode which covers a large area, the charge induced is proportional to the total drift distance of the charges irregardless of whether the charges are actually collected onto the electrode. In the case of pixel electrodes, when a charge is collected it will appear on that single pixel, however, when a charge is trapped the induced charge will be spread out over the electrode surface and will appear on several pixels. In order to achieve the highest possible hit efficiency, the diamond thickness should be optimized to yield the maximum pulse height on the central primary pixel. The current diamond thickness of 500 microns is not optimal for a 125 μm pitch pixel. An essential part of our program in the coming year will be to test comparable diamonds of different thicknesses (300, 400 and 500 microns). Reducing the thickness from 500 microns to 300 microns will reduce slightly the total charge on the surface electrodes. However, the fraction of charge on the central electrode will be increased and simulations show that the charge on the central pixel will be increased.

4.2.2 Efficiency

The efficiency of individual pixels is shown in Fig. 17 where the efficiency is given by the fraction of time that a given pixel or any of its nearest neighbours were above threshold when a track extrapolated to the pixel. There are about 95 tracks in each pixel. The corresponding distribution of pixel efficiencies is shown in Fig. 18. The most probable efficiency is 95 % while there is a tail consisting of a few percent of the pixels which extends down to quite low efficiencies. In order to investigate the low efficiency in the pixels, we plot in Fig. 19 the extrapolated hit position of the tracks for events in which the pixel detector fired. We have thrown out those tracks that extrapolate to the periphery of any pixel ($\pm$7.5 microns). When this is done, it can be seen that the central part of these pixels is completely dead. This

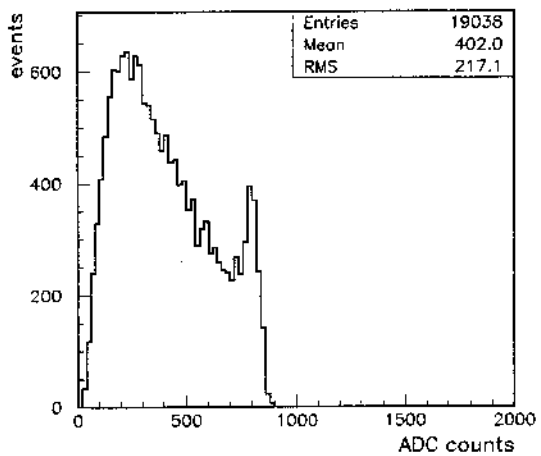

Figure 16: Single pixel pulse height distribution.

indicates the low efficiency pixels have a problem with either the electronics or the bump-bonding. The reason that we see a non-zero efficiency in Fig. 18 for these pixels is because for tracks near the periphery, the neighbouring pixel will, at times, be over threshold. In addition, we find that these same dead pixels do not show any calibration pulse. Taken together this indicates that the failure in these pixels is in the pixel analog circuitry rather than a defect in the bump-bond, metallization, or the diamond itself. The efficiency distribution after removing the 18 dead pixels is shown in Fig. 20. Here the mean efficiency is 94 %.

While still less than 100%, this result is a major breakthrough and clearly demonstrates that diamond pixel detectors are viable. By optimizing the thickness of the diamond as described above, the efficiency should be even further improved.

4.2.3 Spatial Resolution

In order to measure the spatial resolution due to the charge sharing resulting from inclined tracks, the detector was rotated by 15° with respect to normal incidence. At an angle of 15°, with a detector thickness of 500 microns and the pixel lateral size of 125 microns, each track passes under two and only two pixels ($\tan 15° = 125$ microns/500 microns). We define the largest pulse height pixel to be the pixel with the largest pulse height. Fig. 21 shows the distribution of the differences between the track extrapolation point and the center of the primary pixel. The rms is 41 microns which is slightly worse than the digital resolution of 36 microns for 125 micron wide pixels.

We define the two-pixel center-of-gravity by taking the ratio of the pulse height of the largest neighbouring pixel to the pulse height sum of the largest neighbour and primary pixel. This ratio is taken negative if the left neighbour is largest and positive if the right neighbour is largest. This quantity is multiplied by the half width of the pixel, 62.5 microns. In Fig. 22 this center-of-gravity is plotted versus the extrapolated position of the track relative to the center of the primary pixel. Charge sharing is clearly seen in this plot. However, there is a large asymmetry between the left and right sides with the right side showing significantly more correlation with track position than the left. When the particle passes through the detector it is moving from left to right and enters the detector on the side away from the pixel electrodes. As a result, the signal on the left pixel is due largely from charges trapped

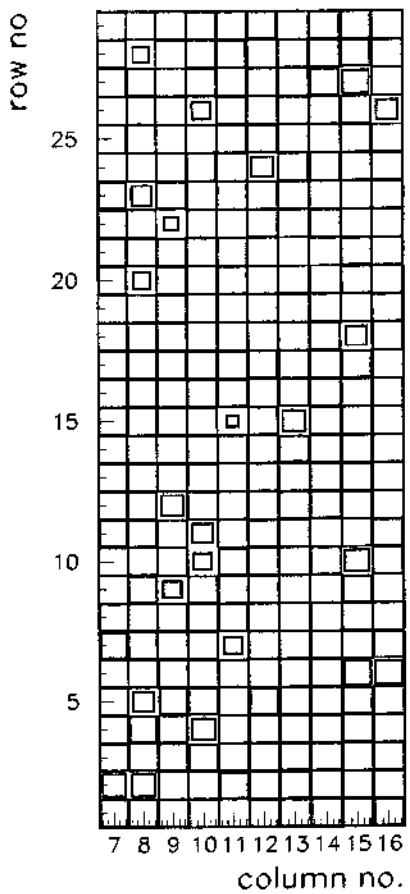

Figure 17: Pixel efficiency map.

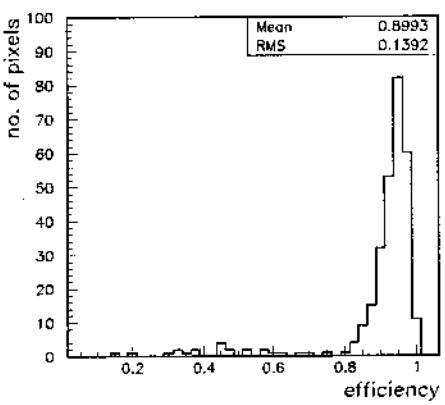

Figure 18: Pixel efficiency distribution.

in the diamond, since they have further to drift to reach the pixel electrodes, whereas the right pixel tends to have more of its signal due to charge collected on the pixel electrode. Here also, optimizing the sensor thickness should improve the performance of the detector.

We calculate a center-of-gravity corrected hit position by x_{cg} = center of primary pixel + CG where CG is the two-pixel center-of-gravity described above. The distribution of the differences between the extrapolated track position and x_{cg} is shown in Fig. 23. The rms of this distribution is 31 microns.

These results are encouraging. The spatial resolution achieved is not what is desired for an LHC pixel detector but improvements are clearly possible. In the coming year, we should have higher quality diamond and we will optimize the thickness of the diamond. Together these should lead to further significant improvement in the spatial resolution approaching that achievable with silicon pixels.

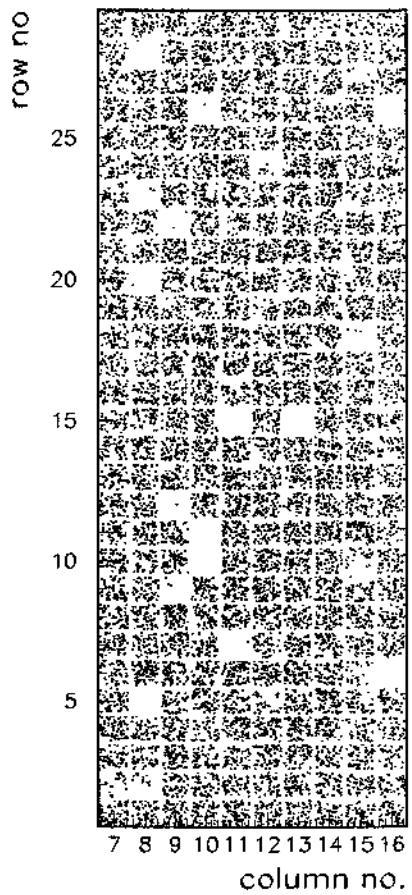

Figure 19: Hit pixels for tracks near center of pixel.

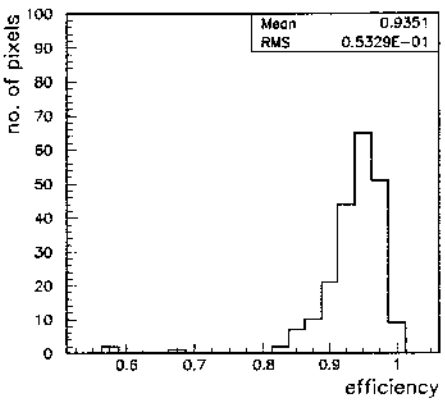

Figure 20: Pixel efficiency distribution after removal of dead pixels.

5 Other Studies and Applications in RD42

5.1 Defect Characterization of Diamond Detectors

The activity of the Florence RD42 group is carried out at the Physics Laboratory of the Department of Energetics (DEF) and at the European Laboratory for Non Linear Spectroscopy (LENS) of the University of Florence. Apart from standard material characterisation as Raman Spectroscopy, X-Ray Diffraction, Scanning Electron Microscopy, it is devoted to the investigation of the native and radiation-induced defects of the RD42 detector prototypes and aimed to relate the trapping and recombination processes with the figures of merit of the diamond-based devices, as charge collection distance, leakage current, width of the pulse height distribution in single-particle experiments. In the last period, thermal spectroscopy methods (Thermally Stimulated Currents Spectroscopy, TSC, Photo-Induced Current Transients Spectroscopy, PICTS, Thermo-luminescence , TL) have been combined together, in a wide range of temperature, to determine shallow and deep trap levels inside the band gap [10]. A continuous distribution of trap levels has been singled out with activation energies ranging from 0.3 to 0.6 eV, and deeper levels from 0.7 to 1.4 eV have also been ascertained [11]. The trap parameters of the main defects have been determined. The effect of the neutron

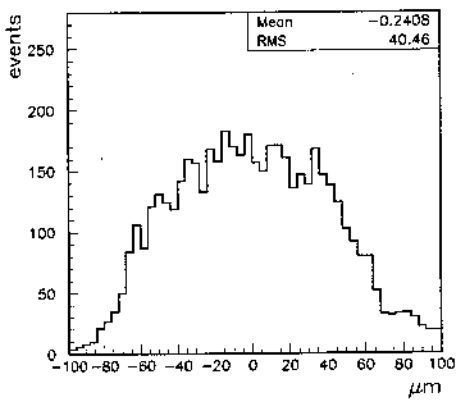

Figure 21: Residual distribution of hit pixel position minus track position.

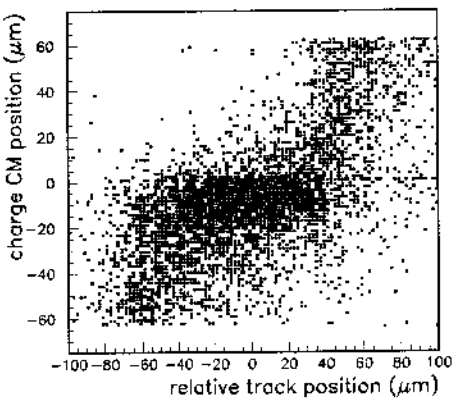

Figure 22: Signal center-of-gravity versus extrapolated track position.

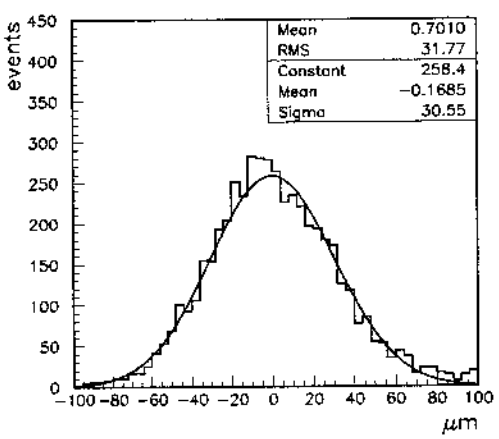

Figure 23: Distribution of extrapolated track position minus x_{cg}, the center-of-gravity corrected hit position.

irradiation has also been studied by use of the cyclotron facility of the Hungarian Academy of Science, at Debrecen Hungary. Up to date samples have been irradiated to level fluences foreseen in the LHC experiments (up to 2×10^{15} n/cm^2). An effect of removal of a main trapping level at 1 eV from the valence band has been assessed [Fig. 24] [12]. The influence of irradiation on more shallow levels is still under study. The trapping defects which are candidate to degrade the lifetime of the carriers are determined by estimating the relative trapping times and comparing them with the collection times of the hole-electron pairs induced by particles. Also the emission coefficient from every single trap is evaluated in order to study the pumping effect, which is believed to be a permanent passivation of the traps, which leads to an increase of the collection efficiency by a factor two. These time constants are known after determination of the activation energy, the capture cross section and the concentration of the trapping centers. Optical spectroscopy analyses have also been performed with excitation over band gap (208 nm wavelength). The free exciton photo-luminescence has been studied as a probe of sample quality [Fig. 25]. Time-resolved spectroscopy has been performed by use of a standard time-correlated single-photon counter with a 100 ps resolution [13]. The time evolution of the 5.25 eV near band-edge exciton has been observed to correlate with the charge collection distance of unirradiated and neutron irradiated de-

tectors. The so-called photoluminescence band A of diamond, peaked at about 2.6 eV, has been observed in all samples and it is believed to be ascribed to mid gap levels which act has recombination centers of carriers. In order to study the influence of the deposition parameters on the quality of diamond a Chemical Vapor Deposition (CVD) method has been developed at DEF. The reactant species, methane and hydrogen, are activated by a DC glow discharge between two electrodes. The substrate where diamond nucleates is mounted on top of the anode and is about 1 cm in diameter. The reactor is a ultra-high vacuum chamber, and a cleaning stage before deposition is performed before deposition by heating the walls under ultra-high vacuum condition.

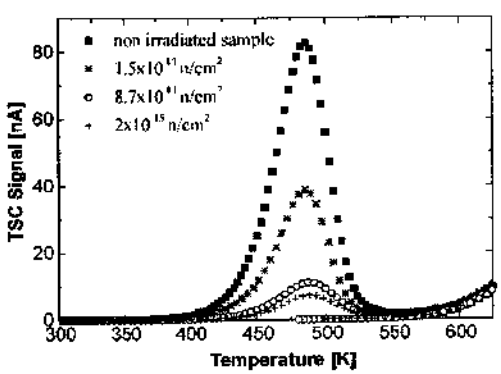

Figure 24: TSC signal vs. temperature for non-irradiated and irradiated CVD diamond samples, taken after a trap filling with a UV Xe-source for 20 min. The samples were biased with 100 V. The heating rate was 0.1 K/s. The neutron fluences are indicated in the legend.

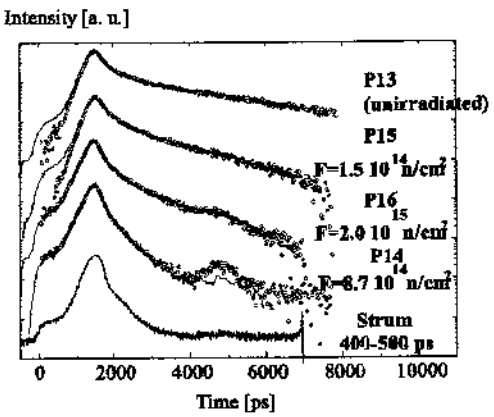

Figure 25: Time evolution of the photoluminescence response of the 5.25 eV exciton peak observed in four CVD diamond samples, unirradiated and irradiated up to 2×10^{15} n/cm^2. The lower line shape is the instrumental broadening. The exciton lifetime decreases after irradiation. This can be correlated to the degradation of the charge collection distance. A decrease in the lifetime of 50 % from the non irradiated to the most irradiated sample corresponds to a decrease of 30 % of the charge collection distance.

5.2 Application of CVD Diamond at DESY

The DESY group is investigating the possibility to use diamond for a low-angle calorimeter for the proposed TESLA project. A detector serving both as a fast luminosity monitor and a low angle calorimeter will be placed at a distance of 220 cm on both sides of the interaction point, covering an annular surface between radii of 1.2 cm and 6.2 cm from the beam line. As a luminosity monitor, the detector will measure the amount of beam induced background particles. About 20000 electron-positron pairs will hit the LCAL on each side of the TESLA detector per bunch crossing, carrying over 20 TeV of energy. The signal left by these particles will be used to resolve luminosity variations within one bunch train. The information will be fed back to the beam delivery system to tune the beam. As a calorimeter, the LCAL will be used to measure electron showers in the region between 6 mrad and 28 mrad. These showers will be used to measure low angle electrons for luminosity measurements and physics studies.

For this purpose, the group is testing the performance of diamond detectors when irradi-

ated with large doses of electromagnetic radiation, of the order of a few MGy. Signal studies for large energy depositions are also underway, with charges ranging from 10^4 electron-hole pairs up to 10^{10}. It is foreseen to use the TTF (TESLA Test Facility) at DESY to study the response of the detectors for very large signals. These tests are also aimed at studying the possibilities of using diamond as a beam profile monitor.

5.3 Application of CVD Diamond at GSI

CVD diamond detectors are in permanent use at GSI by the HADES collaboration, the atomic physics group and the beam diagnostics group. The response of these users is positive. After 2 years of operation, the detectors are working reliable and no damage was reported. Components of diamond detectors to be used in the tumor therapy with ^{12}C ions are in house with final tests expected in March 2001. Demand for more diamond detectors increases.

A new development has been started for CVD diamond strip-detectors to be used as focal plane detectors of magnetic spectrometers. Focal plane detectors are an alternative to gas counters or channel plates. In August 2000 a 200 μm thick CVD diamond strip detector with an area of 60×40 mm^2 has been used as a focal plane detector in a beam-foil experiment aiming to measure the life time of He-like Gold atoms. In order to identify different ionic charge states the diamond strips were read out in coincidence to an X-ray detector.

Investigations of the timing properties of CVD diamond detectors for MIPs were started. A diamond sample and an NE102 plastic scintillator were used in a collimated beam of ^{90}Sr electrons. The time resolution measured using DBAII amplifiers (Diamond Broadband Amplifier, 2.3 GHz) have varied from 280 ps selecting low amplitudes to 95 ps selecting high amplitudes, respectively.

The electronics for very fast pulse counting and data acquisition for the beam-diagnostics diamond detector has been developed. The setup contains newly developed differential discriminators ($<$ 500 ps response time, $>$ 1 GHz trigger frequency) and fast 32-bit counters. The beam-diagnostic detectors allow count rates up to 10^8 particles/s. A new amplifier DBA III (Diamond Broadband Amplifier, 3 GHz) has been developed. Its gain can be matched to the broad dynamic range of heavy-ion signals.

CVD diamond detectors were studied using a ^{12}C micro-beam [14, 15]. A 380 μm thick CVD diamond sample was uniformly irradiated in a ^{12}C micro-beam at 5.9 MeV/amu with a fluence of up to 10^{10} ions/cm^2. Each ^{12}C ion deposited 71 MeV in a depth of 57 μm. Fig. 26 shows the surface topology map obtained from the secondary electron emission spectrum (a) and the map of the charge collection efficiency, CCE, (b) measured in the same region. There are regions in both figures (a) and (b) which are similar. Fig. 26 (c) shows the CCE distribution of the total scanned area (dotted line) and overlayed the distribution from selected 'dark regions'.

6 Proposed Research Program for 2001

The goal of the RD42 research program is to develop best electronic grade CVD diamond and to demonstrate the usefulness and performance of CVD diamond as a radiation sensor material capable of detecting minimum ionizing particles in extremely high radiation environments. In order to achieve this goal the following main program steps had to be performed:

- Characterization of the electrical performance of specific CVD diamond samples grown by De Beers Industrial Diamonds and continuous feed back of results to the manufacturer.

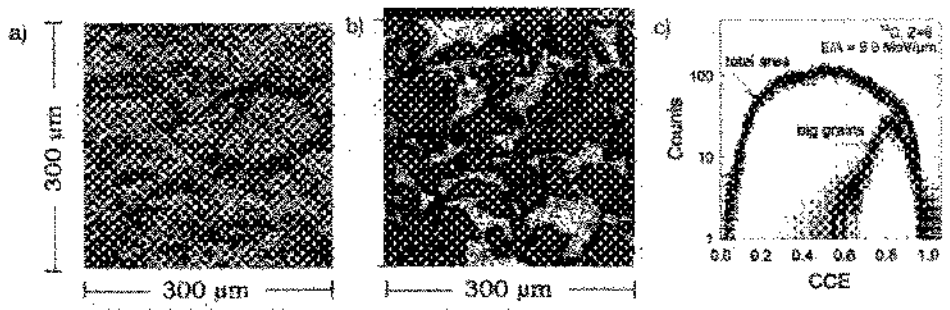

Figure 26: Image from the surface of a CVD diamond obtained by secondary electron emission (left), image from the same region obtained by measuring the charge signal in the micro-beam (middle) and spectra from charge signals for the full region and for selected regions (right).

- Irradiation of samples with π, p and n to fluences up to 5×10^{15} particles/cm^2.
- Material science studies on these CVD diamond samples for defect characterization.
- Test of CVD diamond tracking devices with tailor made radiation hard front-end electronics for strip detectors and pixel detectors, including beam tests.

A big part of this program has been successfully achieved over the last years. Originally it was foreseen to finish the program at the end of 2000. There are however a number of important and decisive measurements still to be performed in this research program. This is partly due to the fact that more critical problems have been encountered than originally foreseen, but even more because there have been delays not under the control of RD42. Some of the major topics which could not be fully treated are the following:

- RD42 has achieved in collaboration with De Beers to have material produced which shows on a regular basis charge collection distances between 200 μm and 220 μm. It has however been recognized that it could be advantageous and possible to produce material with charge collection distances in excess of 250 μm. A special program in form of a research contract - 100 % financed by the US part of RD42 - has been started with De Beers in early 2000 to attempt to produce such material.
- While there have been many promising results from irradiation studies with pions, protons, neutrons, electrons and photons with material of increasing quality, there are more measurements needed for the latest, highest quality CVD diamond samples.
- Material science studies have been pursued in a number of RD42 institutes. New methods and techniques had to be developed specific to CVD diamond. These are now in place, in particular in Florence, and need to be employed to study microscopic effects. This will be very important in view of producing reliably high quality CVD diamond radiation sensors.
- The fast, radiation-hard SCTA128 readout chip developed for diamond strip detectors, in DMILL technology, was submitted into the ATMEL foundry in May 2000 and was expected to be delivered mid August 2000. This run failed completely due to ATMEL technology problems. It was immediately re-submitted by ATMEL for re-processing. It has been finally delivered to CERN in January 2001.

RD42 proposes to concentrate its efforts in 2001 to the following topics

- Pixel prototype detectors, using the top quality CVD material available: implementation of Ti/W contacts and reliable, efficient bump bonding, construction and test of modules with the latest radiation hard ATLAS and CMS front-end chips, and beam test with these modules.
- Characterization of the new, highest quality CVD diamond material produced by De Beers under the existing research contract.
- Proton, neutron and pion irradiations with the highest quality material.
- Carry on with further generic research: study of contacts and the effect of radiation to contacts, study the uniformity of materials, correlation studies with special material science measurements performed by De Beers, and defect characterization of non irradiated and irradiated samples.
- Test of strip detectors with 2×4 cm^2 area with the new, radiation hard SCTA chip from ATMEL (DMILL technology). Eventually also tests with a quarter micron technology full CMOS front-end chip at present under development at CERN.

More details on the planned work program for the pixel test and defect characterization are described in the next paragraphs.

6.0.1 Plans for Future ATLAS Pixel Prototype Tests

There is still room to improve on the ATLAS pixel prototypes we have been able to assemble so far. We must find a reliable way of achieving high quality bump-bonding across the whole face of not only a 1×1 cm^2 prototype sensor, but also pixel module sizes approaching 8×3 cm^2. Indium bump-bonding, such as has been used to produce the CMS diamond pixel prototypes and which was used in the first ATLAS prototype, continues to show promise. With radiation hard pixel readout chips from ATLAS we will be able to "pump-up" the diamond sensors before operating them. With the extra factor of 1.6 in collected charge we expect diamond pixel prototypes with efficiency very close to 100 %. In particular a larger pulse height will reduce the loss of efficiency due to the time walk effect.

We plan to continue this program in the coming year including tests of improved diamond and comparisons of the hit efficiency and spatial resolution with identically configured silicon sensor pixels both before and after irradiations.

6.0.2 Plans for Future CMS Pixel Prototype Tests

Substantial progress and significant breakthroughs have been made in test beam studies of CMS pixels in the past year. This year we plan to build on this momentum. The motivations and milestones for our test beam program in the current year are the following.

- Use higher quality diamond resulting from the De Beers R&D effort to improve efficiency and spatial resolution.
- Optimize the thickness of the diamond to improve efficiency and spatial resolution.
- Compare the performance of the diamond pixels before and after irradiation to several years of LHC pixel operation. (Note that the spatial resolution of diamond strip trackers significantly improves after Mrad of irradiation. Is the same true for the spatial resolution of pixel detectors?)

Ideally, the diamond results should be compared side-by-side with results from identically configured silicon detectors. This will have to wait until 2002 when silicon sensors bonded to the latest version of the CMS readout chip will be available.

6.1 Studies of Defects in CVD diamond

The activities outlined in Sec. 5.1 will be continued during year 2001 on the new generation of top quality samples from De Beers, in order to reach a thorough understanding of the physics of diamond detectors. The final purpose is to determine the trapping levels and the trapping kinetics which limits the charge collection efficiency and rules the effect of pumping. Moreover X-Photo-electron Spectroscopy (XPS) measurements will be performed in order to study the formation of ohmic contacts onto the diamond surface and in particular the formation of the carbide interfaces between the metal coating and the diamond and its relationship with the quality of the contact. The XPS technique has been successfully employed in the past to characterise ohmic and Schottky contacts on diamond [16].

7 Funding and Requests for 2001

As a result of the ongoing progress the RD42 project is supported by many national agencies and the total anticipated funding from sources outside CERN in 2001 is foreseen to be 250 kCHF. One reason why our collaborating institutes obtain national funding is that the RD42 project is officially recognized by CERN within the LHC R&D program. Official recognition of RD42 by CERN with the LHC R&D program has helped in the past to obtain funding from national agencies. For the continuation of the RD42 program as described in section 6 we do not request any direct funds from CERN. We request however that the LHCC officially approves the continuation of the program. This is essential to ensure future funding from national agencies. We estimate that with the presently available manpower a conclusive completion of this program will need further 18 to 24 months. It will be very important for the proposed RD42 program to have access to beam tests. It is foreseen that a minimal infra-structure for sample characterization and beam test preparation is maintained at CERN. This will be a part of an EP division common project. The facility will be mainly used by external RD42 collaborators. We therefore request

- Three 7-day testbeam running periods per year for the duration of the project, of which one could be parasitic to other users.
- Maintain the present 20 m^2 of laboratory space for test setups, detector preparation and electronics development.
- Maintain the present minimal office space for full time residents and visiting members of our collaboration.

8 Publications and Talks given by RD42

8.1 Talks since 1998

1. Vienna Wire Chamber Conference, Vienna, 1998
2. 2nd Int. Conf. on Radiation Effects in Semiconductor Materials, Detectors and Devices, Florence, 1998 (2 talks)
3. Pixel 98, FNAL, 1998 (2 talks)
4. VERTEX 98, Santorini, 1998
5. 6th Int. Conf. on New Diamond Sci. and Techn., Pretoria, 1998
6. 6th Int. Workshop on GaAs and Related Compounds, Prague, 1998
7. 6th Int. Conf. on Advanced Technology and Particle Physics, Como, 1998 (two talks)
8. VERTEX 99, Texl, Netherlands, 1999
9. 10th European Conf. on Diamond and Related Materials, DIAMOND 99, Prague, 1999
10. 7th Int. Conf. for Colliding Beam Physics, INSTR 99, Hamamatsu, 1999
11. 3rd Int. Conf. on Radiation Effects on Semiconductor Materials, Detectors and Devices (RESMDD), Firenze, 2000 (3 talks).
12. Pixel2000, Genoa, 2000.
13. Vertex2000, Michigan, 2000.
14. ICHEP, Osaka, 2000.
15. DPF-Meeting of the American Phys. Soc., Columbus, 2000

8.2 Publications since 1999

1. D. Meier *et al.* (RD42 Collaboration), "Proton Irradiation of CVD Diamond Detectors for High Luminosity Experiments at the LHC", CERN-EP/98-79, Nucl. Instr. Meth. **A426** (1999) 173.

2. R. Wedenig *et al.* (RD42 Collaboration), "CVD Diamond Pixel Detectors for LHC Experiments" Nucl. Phys. **B78** (1999) 497-504.

3. E. Berdermann *et al.*, "First Applications of CVD-Diamond Detectors in Heavy-Ion Experiments", Nucl. Phys. (Proc. Suppl.) **B78** (1999) 533-539.

4. F. Hartjes *et al.* (RD42 Collaboration), "Parametrisation of radiation effects on CVD diamond for proton irradiation", Nucl. Phys. **B78** (1999) 675.

5. S. Schnetzer *et al.* (RD42 Collaboration), IEEE Trans. Nucl. Sci. **46** (1999) 3.

6. W. Adam *et al.* (RD42 Collaboration), "Review of the Development of Diamond Radiation Sensors", Nucl. Instr. Meth. **A434** (1999) 131-145.

7. M. Friedl *et al.* (RD42 Collaboration), "CVD Diamond Detectors for Ionizing Radiation" Nucl. Instr. Meth. **A435** (1999) 194.

8. W. Adam *et al.* (RD42 Collaboration), "The First Bump-Bonded Pixel Detectors on CVD Diamond", Nucl. Instr. Meth. **A436** (1999) 326-335.

9. W. Adam *et al.* (RD42 Collaboration), "Pulse height distribution and radiation tolerance of CVD diamond detectors" Nucl. Instr. Meth. **A447** (2000) 244.

10. W. Adam *et al.* (RD42 Collaboration), "Micro-Strip Sensors based on CVD Diamond", Nucl. Instr. and Meth. **A453** (2000) 141-148.

11. W. Adam *et al.* (RD42 Collaboration), "Radiation Tolerance of CVD Diamond Detectors for Pions and Protons", Proc. RESMDD in Florence (2000). submitted for publication in Nucl. Instr. Meth. (2000).

12. W. Adam *et al.* (RD42 Collaboration), "Performance of Irradiated CVD Diamond Micro-Strip Sensors", accepted for publication in Nucl. Instr. Meth. (2000), CERN-EP-200-115.

13. W. Adam *et al.* (RD42 Collaboration), "Diamond Pixel Detectors", Proc. of Pixel2000, submitted to Nucl. Instr. Meth. (2000).

14. R. Stone *et al.* (RD42 Collaboration), "Diamond Pixel Detector Development", submitted to Nucl. Instr. Meth. (2000).

15. S. Schnetzer *et al.* (RD42 Collaboration), "Diamond Pixel Detectors", Proc. of ICHEP (2000).

References

[1] "Minutes of the 44. CERN LHCC Meeting", 10. Feb. 2000, CERN/LHCC 2000-006.

[2] W. Adam *et al.* (RD42-Collaboration). "Development of Diamond Tracking Detectors for High Luminosity Experiments at the LHC". Status Report/RD42, CERN/LHCC 2000-011, CERN/LHCC 2000-015, (2000).

[3] De Beers Industrial Diamond Division. Charters, Sunninghill, Ascot, Berkshire, SL5 9PX England.

[4] Integrated Detector and Electronics (IDE) AS. "The VA Circuits". `www.ideas.no`. Pb.315, Veritasveien 9, N-1322 Hovik, Norway.

[5] D. Meier. *"CVD Diamond Sensors for Particle Detection and Tracking"*. PhD thesis, University of Heidelberg and CERN, `atlasinfo.cern.ch/Atlas/documentation/thesis/thesis.html`, (1999).

[6] W. Adam *et al.* "Micro-Strip Sensors based on CVD Diamond". *Nucl. Instr. Meth.*, **A453** (2000), or CERN-EP-2000-041.

[7] D. Meier *et al.* (RD42-Collaboration). "Proton Irradiation of CVD Diamond Detectors for High Luminosity Experiments at the LHC". *Nucl. Instr. Meth.*, **A426** (1999) 173.

[8] W. Adam *et al.* "Performance of Irradiated CVD Diamond Micro-Strip Sensors". *Nucl. Instr. Meth.*, (2001), or CERN-EP-2000-115.

[9] W. Adam *et al.* "First Bump-Bonded Pixel Detectors on CVD Diamond". *Nucl. Instr. Meth.*, **A436** (1999) 326-335.

[10] M. Bruzzi *et al.* "Photo-induced Deep Level Analysis in Undoped CVD Diamond Films". *Diamond and Related Materials*, **9** (2000) 1081-1085.

[11] E. Borchi *et al.* "Photo-induced Current Spectroscopy in Undoped CVD Diamond Films". *Mat. Res. Soc. Symp. Proc.*, **588** (2000) 277.

[12] M. Bruzzi *et al.* "Electrical Properties and Defect Analysis of Neutron Irradiated Undoped Diamond Films". *Diamond and Related Materials*, (in press).

[13] F. Bogani *et al. Phys. Stat. Sol.*, **A181** (2000) 23-27.

[14] E. Berdermann *et al.* "Recent Results from CVD-Diamond Heavy-Ion Detectors". *Proc.* 38th *Int. Winter Meeting on Nucl. Phys.*, Bormio, (2000).

[15] E. Berdermann *et al.* "The Use of CVD-Diamond for Heavy-Ion Detection". *Proc.* 7th *Int. Conf. Diamond Sci. Techn. (ICNDST-7)*, Hong-Kong, (2000).

[16] T. Tachibana *et al. Phys. Rev.*, **B45** (1992) 968.